applied sciences

MDPI

Article

Determination of Geometrical REVs Based on Volumetric Fracture Intensity and Statistical Tests

Ying Liu [1], Qing Wang [1], Jianping Chen [1,*], Shengyuan Song [1,2], Jiewei Zhan [1] and Xudong Han [1]

[1] College of Construction Engineering, Jilin University, Changchun 130026, China; liuying01tg@126.com (Y.L.); wangqing@jlu.edu.cn (Q.W.); songshengyuan@126.com (S.S.); zhanjwtg@126.com (J.Z.); hanxd15@mails.jlu.edu.cn (X.H.)

[2] College of Earth Sciences, Jilin University, Changchun 130026, China

* Correspondence: chenjpwq@126.com

Received: 6 April 2018; Accepted: 14 May 2018; Published: 16 May 2018

Abstract: This paper presents a method to estimate a representative element volume (REV) of a fractured rock mass based on the volumetric fracture intensity P_{32} and statistical tests. A 150 m × 80 m × 50 m 3D fracture network model was generated based on field data collected at the Maji dam site by using the rectangular window sampling method. The volumetric fracture intensity P_{32} of each cube was calculated by varying the cube location in the generated 3D fracture network model and varying the cube side length from 1 to 20 m, and the distribution of the P_{32} values was described. The size effect and spatial effect of the fractured rock mass were studied; the P_{32} values from the same cube sizes and different locations were significantly different, and the fluctuation in P_{32} values clearly decreases as the cube side length increases. In this paper, a new method that comprehensively considers the anisotropy of rock masses, simplicity of calculation and differences between different methods was proposed to estimate the geometrical REV size. The geometrical REV size of the fractured rock mass was determined based on the volumetric fracture intensity P_{32} and two statistical test methods, namely, the likelihood ratio test and the Wald–Wolfowitz runs test. The results of the two statistical tests were substantially different; critical cube sizes of 13 m and 12 m were estimated by the Wald–Wolfowitz runs test and the likelihood ratio test, respectively. Because the different test methods emphasize different considerations and impact factors, considering a result that these two tests accept, the larger cube size, 13 m, was selected as the geometrical REV size of the fractured rock mass at the Maji dam site in China.

Keywords: REV; fractured rock mass; likelihood ratio test; Wald–Wolfowitz runs test; Maji hydropower station

1. Introduction

There are many discontinuities in fractured rock masses, and the structural characteristics (such as joint orientation, spacing, spatial distribution, and combination condition) control the mechanical properties, the deformation, and the failure behavior of rock masses. Discontinuities are also the source of the anisotropy and inhomogeneity of rock masses. The size effects of the mechanical and geometrical properties of a rock mass are prominent; the parameters of a rock mass will change gradually as the research scope changes. When the rock mass size is larger than or equal to a certain value, the fluctuation of rock properties significantly decreases; the continuum method can be used to perform a numerical analysis; and the equivalent continuum parameters can represent the properties of the rock masses. Accordingly, this critical cube size is defined as the representative element volume (REV) [1]. Thus, it is important to accurately determine the equivalent hydraulic, mechanical and geometrical parameters when analyzing the properties of rock masses.

The concept of REV was presented in the study of porous media seepage [2]. Subsequently, research on REVs has been carried out in various fields. Long et al. [3] generated a 2D fracture system to study the equivalent permeability of fractured rock masses. Kulatilake and Panda [4] and Wang et al. [5] used the permeability coefficient and the equivalent permeability tensor to evaluate the REV size in the field of rock seepage. The REV size of porous media has been estimated based on X-ray micro computed tomography (micro-CT) [6–8]. Tóth and Vass [9] estimated the REV size of the fractured rock mass based on fracture network modeling tools (REPSIM code) and geometrical parameters (such as the fractal dimension of the fracture midpoints, length exponent, and relative dip) and analyzed the relationship between the size of percolation clusters and REVs at a study site in the Pannonian Basin. In the field of rock mechanics, Neuman [10] and Pinto and Da [11] adopted an in situ test method to obtain the REV size of rock masses, but this method was limited by site conditions and high costs. Subsequently, the finite element method was developed to study the size effect of a rock mass and to explore the REV size of a jointed rock mass [12,13]. By considering numerical homogenization (NH) and the geometrical approach, the mechanical REV was discussed by Chalhoub and Pouya [14]. Castelli et al. [15] used the displacement discontinuity method to discuss the scale effects of rock masses. With the innovation of research technology, the distinct element method was developed to discuss REV size and to study the size effect of REVs based on the equivalent elastic compliance tensor, fracture length, fracture aperture, deformation modulus, and Poisson's ratio of fractured rock masses [16–18]. Recently, the REV was also studied in the field of damage mechanics. By considering joint aperture and roughness, Ni et al. [19] used the damage coefficient to determine the REV size. Li and Tang [20] established a mesoscopic constitutive law of REV based on a statistical meso-damage mechanical method (SMDMM) to simulate the rock failure process.

In addition to numerical methods, statistical methods are also widely applied to study the REV size. Lu et al. [21] determined REV size by using a fractal geometry method based on the evaluation of the statistical homogeneity of the structure of a rock mass. Pierce et al. [22] introduced a method using Particle Flow Code to explore REV size based on a 3D fracture network model. Esmaieli et al. [23] determined a geometrical REV and mechanical REV using the T test and the F test; the mechanical REV size was larger than the geometrical REV size. Xia et al. [24] analyzed REV size by considering the blocky structure of a fractured rock mass using the GeneralBlock program. The relationship between REV size and average joint trace length was discussed by various scholars. Oda [25] suggested that REV size should be three times greater than the typical joint trace length and proposed to determine REV size by using a crack tensor. According to Li and Zhang [26], an REV size should be approximately five times the average crack length. Another size was proposed by Lama and Vutukuri [27]: ten times the mean joint length. On the other hand, the relationship between REV size and joint spacing was established by other researchers [13,24,28].

The complexity of rock mass structure characteristics (such as anisotropy, inhomogeneity, and discontinuity) and the limitation of acquiring several parameters (such as the number of fractures, fracture orientation, fracture trace length, fracture width, fracture fill, and ground water flow) have restricted the development of rock mechanics. However, with the development of the computer and mathematical theory, the discontinuities of rock masses have been described in detail with 3D fracture network modeling technology [29–31]. Subsequently, some scholars have conducted research on geometrical REVs using 3D fracture network models.

Zhang et al. [32–34] introduced some methods to determine the geometrical REV size using a 3D fracture network model and statistical test methods: A 3D fracture network model was established, and the simulated rock masses were divided into cubes of the same size, which varied from 1 to 20 m. Then, the parameters of the rock mass were statistically calculated. Finally, the REV size was determined by the Kolmogorov–Smirnov (KS) and the Wilcoxon rank-sum tests. Zhang et al. [35] utilized a contingency table method to analyze the geometrical parameters of fractures (such as fracture density, length, dip direction, and dip angle) and to ascertain the geometrical REV size based on a 3D

fracture numerical network modeling. Song et al. [1] and Li et al. [36] considered the discontinuity connectivity to analyze the geometrical REV size at the Songta dam site in China.

In this study, the joint data were collected from the abutment rock mass of the Maji hydropower station. The field survey shows that the abutment rock masses are relatively intact. The fractures with one end censored and both ends observable are the most common and the fracture diameters are relatively small. The rock masses were not strongly affected by a certain tectonic activity. According to the abovementioned fact-finding, the regional fractures were clearly divided into four sets. The K-S goodness-of-fit tests indicate that the fracture spacing of each fracture set obeys a negative exponential distribution. Therefore, a homogeneous Poisson progress could simulate the locations of fracture centroids. To comprehensively consider the anisotropy of rock masses, simplicity of calculation and comprehensive differences between different methods, the volumetric fracture intensity P_{32} and two statistical test methods were employed to estimate the REV sizes. The purpose of this paper is to introduce a new method for determining the geometrical REV size of the entire rock mass based on the volumetric fracture intensity P_{32} and statistical tests. The volumetric fracture intensity P_{32} was calculated based on the randomness of the distribution of the cubes in a 3D fracture network model. The probability distribution, size effect, and spatial effect of the volumetric fracture intensity P_{32} at the Maji dam site in China were studied. Finally, the size of the geometrical REV was assessed based on the P_{32} values, likelihood ratio test and Wald–Wolfowitz runs test in the study area.

2. The Establishment of a 3D Fracture Network Model

2.1. Data Collection from the Study Area

In this study, the Maji hydropower station dam site was used as a study area, and the REVs of fractured rock masses were discussed based on the volumetric fracture intensity P_{32} and two statistical tests. The Maji hydropower station is located in the middle and lower reaches of the Nu River in China (Figure 1). A 290-m-high concrete arch dam, which has a hydroelectric generating capacity of 4200 MW, is planned for this site. An approximate mountain–canyon topography is present at the dam site area; the difference in the bank slope elevation is generally above 2000 m, and the riverbed elevation ranges from 1320 to 1403 m.

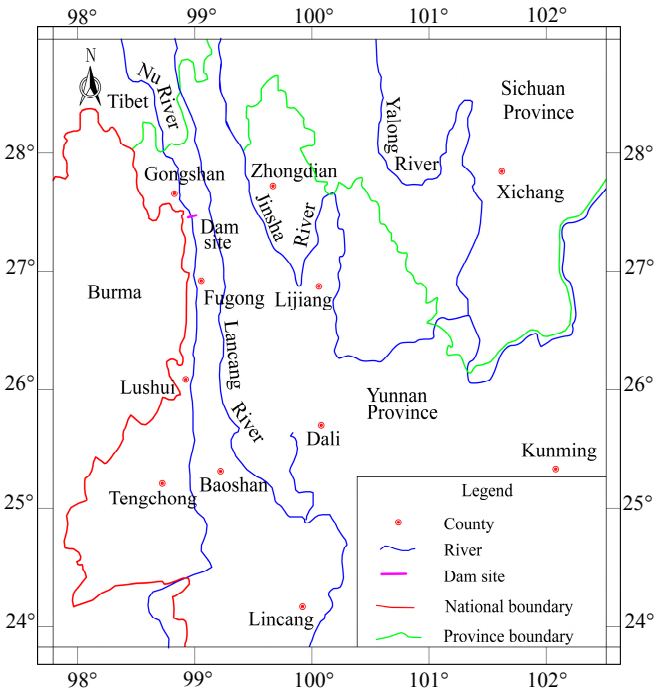

Figure 1. The location map of the Maji dam site area.

The 12,339-m-long tunnel that is located on both sides of the dam site was surveyed. The results indicated that the mixed granite and mixed gneiss, which are more than 400 m thick, have a lenticular grain structure and are exposed in the right bank slope; the general orientation of the gneissosity is 330°N–340° W/SW∠75–85°. Neither a large-scale fault nor a fault zone is located on either bank. Fractures with steep dip angles are better developed, while others with low dip angles are less developed. Except for the fractures that were located in the strong unloading zones and weak unloading zones and were located near large faults, the fractures are commonly closed. A few joints were filled with papery rock debris, the others had sparse black mica precipitation.

Tunnel PD222, which is striking northwest and located in the right bank slope, is almost orthogonal to the Nu River. The 979 fracture data points from five tunnels near tunnel PD222 were surveyed by the rectangular window sampling method and included data such as orientation, coordinates, trace length, fill and ground water [37]. In this study, due to engineering requirements, tunnel PD222 was used as the main research object, and the 2D fracture traces are described in Figure 2. Of all the data, 213 fracture data points, including fracture orientation, trace length, and fracture spacing, were selected to generate a 3D fracture network model for engineering purposes.

Figure 2. The illustration of the 2D joint traces.

2.2. 3D Fracture Network Modeling

A 3D fracture network model was generated based on the following two assumptions [38–40]:

1. The discontinuities are thin planar discs with a random distribution.
2. The fractures are not open; water and fracture fill can be disregarded.

The simulation procedure was described as follows:

1. Determination of the statistical homogeneity

Because limited joints are located in the tunnel, the division of statistical homogeneity would reduce the number of statistical samples and affect the accuracy of the fracture simulation results. Furthermore, the 3D fracture network model generated by the inhomogeneity of the joint data can meet engineering needs. Therefore, the entire joint dataset is considered to be statistically homogeneous to generate a 3D fracture network.

2. The discontinuity orientation data simulation

The joint data were divided into four sets based on the fracture orientations in tunnel PD222 using the modified K-means algorithm introduced by Li et al. [41]. The results are shown in Table 1 and Figure 3. As shown in Table 1, some of the fracture sets were identified based on the relatively few fracture data points available. To ensure the reasonableness and reliability of the identified fracture sets, the regional fracture data (i.e., the fractures collected from five tunnels near tunnel PD222) were divided into four different fracture sets using the method proposed by Li et al. [41]. As shown in Figure 4, the dataset of the fractures with steep dip angles is larger than that of the fractures with low dip angles. The mean orientation of each fracture set for tunnel PD222 and that of the corresponding regional fracture set are similar. Subsequently, the statistical similarity between the regional joint data of each fracture set and the corresponding joint data obtained from PD222 was determined by using KS tests. As a result, the identified fracture sets based on the data obtained from tunnel PD222 were reasonable, reliable, and statistically significant.

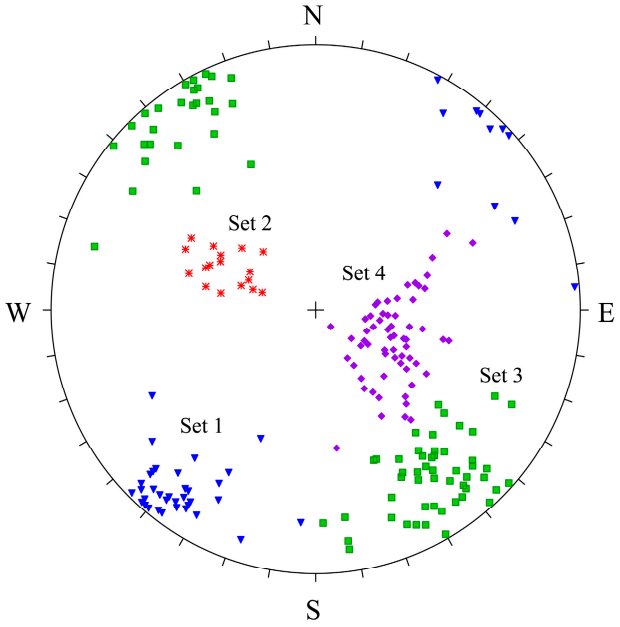

Figure 3. The poles of the fracture orientations on the upper hemisphere for each fracture set.

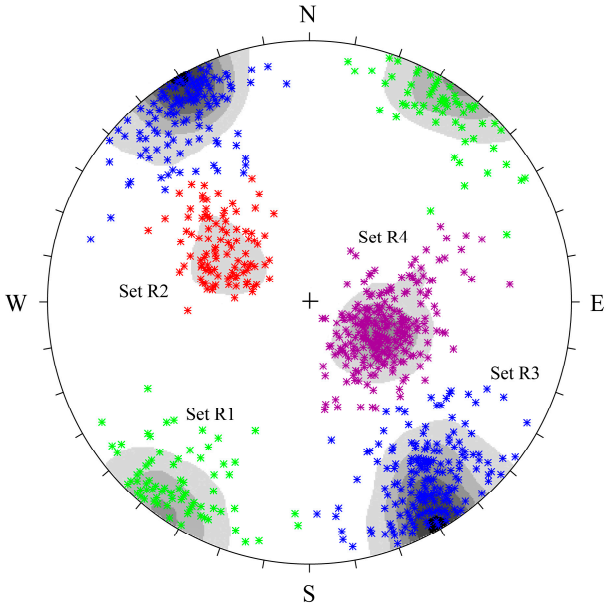

Figure 4. Equal-area projection diagram for fracture sets located in the dam site area.

In theory, the joint orientations of each fracture set can be determined by a Fisher distribution, Bingham distribution, bivariate normal distribution, or bivariate empirical distribution [40,42–45]. However, due to the complexity of the geological structure and investigation error, it is very difficult to determine a distribution that precisely fits the fracture set data. Therefore, considering goodness-of-fit and simple calculation, the Fisher distribution and bivariate empirical distribution were generally used to describe the distribution of the fracture orientations. In this work, the bivariate empirical distribution was used to depict the fracture orientation distributions of each fracture set [46].

3. Bias correction on orientations of the discontinuities

The weighting function W_i of the discontinuities was calculated to correct the orientation sampling bias of the sampling windows [47].

$$W_i = \left[\left(\cos^2 \theta_i \sin^2 \beta_i + \cos^2 \beta_i \right)^{1/2} + \frac{\pi d_i}{4h} \cos \beta_i \sin \theta_i + \frac{\pi d_i}{4w} \cos \theta_i \right]^{-1} \quad (1)$$

where w and h represent the width and height of the sampling window, respectively; θ_i represents the dip angle of the discontinuity i; β_i represents the angle between the strike of the sample plane and the dip direction of the discontinuity i; and d_i represents the diameter of discontinuity i.

4. Discontinuity geometry simulation

The discontinuity geometry simulation includes a trace length simulation and diameter simulation. For the trace length simulation, due to the sampling deviations of the trace lengths in the field, the observed trace lengths should be corrected before generating the disc diameter by using the method introduced by Kulatilake and Wu [37]:

$$\mu = \frac{wh(1 + R_0 - R_2)}{(1 - R_0 + R_2)(w \int_0^{\pi/2} g(\theta) \sin \theta d\theta + h \int_0^{\pi/2} g(\theta) \cos \theta d\theta)} \quad (2)$$

where w and h represent the width and height of the sampling window, respectively; R_0 and R_2 are the fractions of joints with both ends unobservable and both ends observable in the sampling window, respectively; θ is the dip angle of the joint disc; and $g(\theta)$ is the probability density function of dip angle θ. A goodness-of-fit test (Kolmogorov–Smirnov) was utilized to determine the optimal probability distribution of the observed trace length. In this section, we assume that the same distribution form and standard deviation can be used for the observed trace length and the corrected trace length. In this paper, for the simulation of the fracture diameter, the fracture is assumed to be a thin planar disc. Based on the stereological relationship between the distribution of the corrected trace length and disc diameter [48], the fracture diameter of each fracture set was identified using the method proposed by Zhang and Einstein [49]. The results are shown in Table 1.

5. Simulation of the discontinuity intensity and location

The 2D fracture network was generated based on the fracture information (such as joint trace coordinate, dip direction, and dip angle) obtained from the sampling window. The normal fracture frequency of each fracture set could be calculated based on scanlines generated in the 2D fracture network [50]. The volumetric fracture intensity of each fracture set could be determined [49,51–54] (Table 1). Based on the KS goodness-of-fit tests, a negative exponential distribution could accurately fit the fracture spacing of each fracture set. As a result, the location of each fracture centroid could be obtained by using a homogeneous Poisson progress [46,53,55,56].

6. Monte-Carlo simulation and validation

A 150 m × 80 m × 50 m 3D model size was designed for engineering purposes. The 3D fracture network model was established based on the volumetric fracture intensity P_{32} and the model size. Based on the abovementioned parameters (such as fracture orientation, fracture diameter, and fracture location) and the corresponding statistical distributions, more 3D fracture network models were generated according to the Monte-Carlo simulation method [46].

An important concern is whether the generated fracture networks can represent the actual field conditions. Therefore, a model validation procedure was implemented based on the fracture parameters in the 2D cut plane to determine the optimal model from the many generated network models. Finally, an optimal model was selected from the many accepted models according to the method of Esmaieli et al. [23], as reported in Table 2.

Table 1. Parameters for the 3D fracture network modeling.

Fracture Set	Fracture Number	Mean Orientation		Measured Mean Trace Length (m)	Corrected Trace Length			Fracture Diameter			P_{32} (m^2/m^3)
		Dip Direction (°)	Dip Angle (°)		Mean (m)	Std. (m)	Distribution Type	Mean (m)	Std. (m)	Distribution Type	
1	49	219.37	85.15	1.38	1.94	0.73	Gamma	2.16	0.64	Gamma	0.462
2	18	294.00	41.48	1.42	2.16	1.13	Gamma	2.26	1.31	Gamma	0.223
3	79	144.53	83.49	1.23	1.79	0.74	Gamma	1.80	0.55	Gamma	2.179
4	67	111.23	36.08	1.50	2.29	0.98	Gamma	2.35	0.88	Gamma	0.826

Table 2. Parameter comparison between the measured data and simulated data obtained from the optimal model.

Fracture Set		Fracture Number	Mean Fracture Orientation		Trace Length		Trace Type			Spherical Variance	K
			Dip Direction (°)	Dip Angle (°)	Measured	Corrected	R_0	R_1	R_2		
1	Measured	49	219.37	85.15	1.38	1.94	0.18	0.55	0.27	0.058	16.35
	Simulated	49	224.90	87.10	1.31	1.79	0.09	0.63	0.28	0.059	16.62
2	Measured	18	294.00	41.48	1.42	2.16	0.17	0.50	0.33	0.051	18.80
	Simulated	19	295.60	40.50	1.63	2.06	0.12	0.62	0.26	0.053	19.10
3	Measured	79	144.53	83.49	1.23	1.79	0.19	0.54	0.27	0.025	38.44
	Simulated	79	141.90	83.30	1.31	1.63	0.13	0.65	0.22	0.025	38.40
4	Measured	67	111.23	36.08	1.50	2.29	0.08	0.46	0.46	0.072	23.81
	Simulated	67	111.10	32.10	1.69	2.03	0.01	0.60	0.39	0.073	26.40

3. Methodology

A statistical test is a method of statistical inference. Commonly, two statistical datasets are compared, or a set of data obtained from a field survey is compared against a synthetic dataset from an idealized model. In this study, the likelihood ratio test and Wald–Wolfowitz runs test were performed to describe the statistical similarity of the two sample datasets, which were obtained from different cube sizes in the 3D fracture network model, and to determine an REV size at the Maji dam site.

3.1. Likelihood Ratio Test

In statistics, a likelihood ratio test is a statistical test used for comparing the goodness-of-fit of two samples. The key of a hypothesis test is the method used to determine the statistics; the statistic λ can be obtained by Huelsenbeck and Crandall [57]:

$$\lambda = \frac{L_0(x_1, \ldots, x_n)}{L_1(x_1, \ldots, x_n)} = \frac{\sup_{\theta \in \Theta} L_0(x_1, \ldots, x_n; \theta)}{\sup_{\theta \in \Theta} L_1(x_1, \ldots, x_n; \theta)} \tag{3}$$

where $L_0(x_1, \ldots, x_n; \theta)$ and $L_1(x_1, \ldots, x_n; \theta)$ are the likelihood functions, sup is the supremum function, $x_1, \ldots, x_n$ represent the observations of the sample, and θ represents a notional parameter.

To quickly obtain the statistic λ, a convenient method was proposed by Wilks [58]:

$$-2 \ln \lambda = x^2 \tag{4}$$

where $-2 \ln \lambda$ is an approximately x^2 distribution under the null hypothesis when the sample size n approximates ∞.

The critical test statistic λ_α is determined based on a threshold level α that is obeyed by a x^2 distribution and Equation (4), and the p value is determined by

$$p = p(\lambda \geq \lambda_\alpha) \tag{5}$$

When the p value is greater than or equal to the significance level α, the two samples are considered statistically similar. Commonly, a 5% significance level is defined as a threshold in the likelihood ratio test to obtain a geometrical REV size for a fractured rock mass.

3.2. Wald–Wolfowitz Runs Test

The Wald–Wolfowitz runs test is a nonparametric statistical test that checks a randomness hypothesis for a two-valued data sequence [59]. In this test, two random samples (X and Y) from different populations with different continuous cumulative distribution functions are obtained; the samples X and Y involve m observations and n observations, respectively. The procedure of the Wald–Wolfowitz runs test is as follows:

1. The merged samples X and Y are sorted in ascending order, and sample X is coded as a "1", while sample Y is coded as a "2".
2. Each observation is replaced by a label, "1" or "2", depending upon the sample to which it originally belonged.
3. Calculate the number (run) of a consecutive sequence of identical labels ("1" or "2").
4. To determine the test statistic, when both m and n are less than or equal to 20, the test statistic is the total number of runs, U. The critical value U is obtained from the table of the Wald–Wolfowitz runs test. When the number of observations is larger than 20, U follows a normal distribution asymptotically. The expected number of runs and variance are given as

$$E(U) = \frac{2mn}{m+n} + 1 \tag{6}$$

$$Var(U) = \frac{2mn(2mn - m - n)}{(m+n)^2(m+n-1)} \tag{7}$$

The test statistic Z is given by Friedman and Rafsky [60]:

$$Z = \frac{U - E(U)}{\sqrt{Var(U)}} \tag{8}$$

5. The p value is calculated based on the small U value or the test statistic Z obtained from the normal distribution. In this study, the REV size of a rock mass was determined based on the statistical similarity between two compared samples. When the significance level p values exceed a threshold level of 0.05, the fluctuation in P_{32} values significantly decreases as the sample size increases, and the P_{32} values of two compared samples are considered statistically similar. To better demonstrate the procedure of detecting the REV size by using these two statistical test methods, a calculation flow chart is provided in Figure 5.

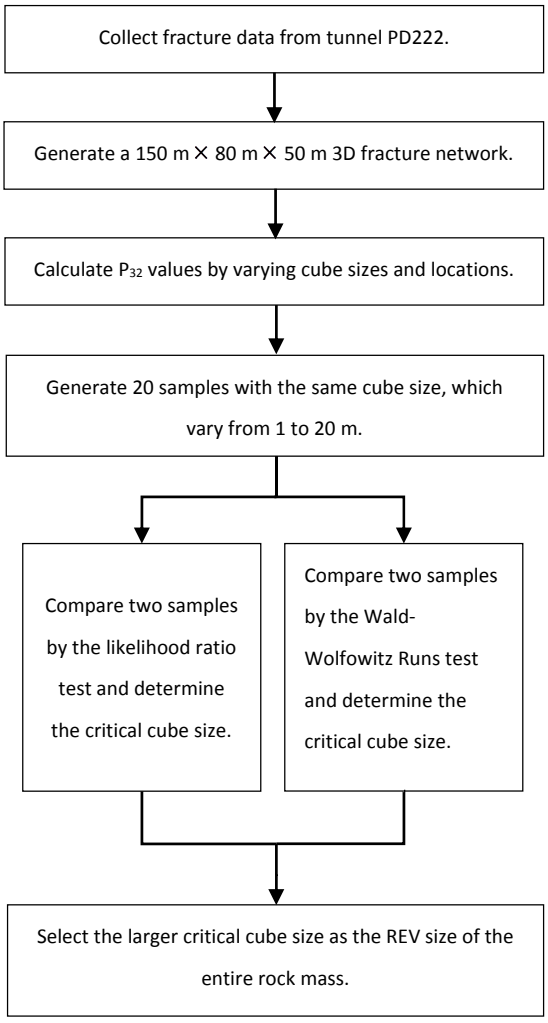

Figure 5. Flow chart of statistical tests for determining the REV size.

4. Determination of the Geometrical REV

The natural internal features of fractured rock masses could be better reflected by establishing a 3D fracture network model in this work. Then, we could more easily analyze the geometrical properties

of fractured rock masses with the generated 3D fracture network model. In this study, the REV size of jointed rock masses was defined by the volumetric fracture intensity P_{32} (area of fractures per unit volume of rock mass) and two statistical test methods.

4.1. P_{32} Characteristics

The volumetric fracture intensity, which is the most useful measure of discontinuity intensity, indicated by the quantity P_{32}, is a fraction expressing the area of fractures per unit volume of rock mass and is used in the 3D fracture network model [54]. In this work, the Delaunay triangulations algorithm was utilized to calculate the P_{32} value, and the calculation procedure was described in detail by Zhan et al. [61].

In this paper, considering the influence of the boundary effect, a 140 m × 70 m × 40 m fracture network model was applied to calculate the volumetric fracture intensity P_{32} and to determine the REV size based on the statistical tests. A total of 100 sets of cubes were selected from the generated 3D fracture network model (Figure 6), and the cube size of each set ranged from 1 to 20 m, changing at an increment of 1 m; then, the P_{32} values were calculated using the method of Zhan et al. [61]. In this study, the P_{32} values from cubes of the same side length were selected as a dataset in the 3D fracture network model. As a result, 20 random datasets, which included 100 random data points (P_{32}) in each dataset, were established. The dataset with cube size of *i* m was defined as sample *i*. The selected random cube sizes varied from 1 to 20 m. Therefore, the 20 samples, from 1 to 20, were generated based on the aforementioned procedure. The chi-square test was used to evaluate whether the P_{32} values for each sample obey a certain distribution. Several probability density distribution forms (such as uniform, normal, negative exponential, lognormal, gamma, beta, binomial, Poisson, and triangle distribution) were checked using the chi-square goodness-of-fit tests to obtain the optimal distribution of the P_{32} values. The results of the chi-square goodness-of-fit tests are illustrated in Table 3. Table 3 shows that the distribution forms of the P_{32} values for each sample are different at a significance level of 0.05. The frequency histograms of the P_{32} values for cube sizes of 3, 10, and 15 m are shown in Figure 7. As shown in Figure 7a, the P_{32} values follow a gamma distribution when the cube size is 3 m, and Figure 7b,c shows that a normal distribution can be used for cube sizes of 10 m and 15 m.

The 100 selected sets of P_{32} values for cube sizes ranging from 1 to 20 m are shown in Figure 8. The size effects were clear, and the P_{32} values change with the spatial positions of cubes. When the cube size is smaller, the distribution of the volumetric fracture intensity P_{32} values is discrete, the difference between the maximum and minimum values is significant, the fluctuation in P_{32} values is greater, and the spatial effect is obvious. When the cube size increases, the maximum value of the P_{32} decreases and the minimum value of P_{32} increases, the difference between the maximum and minimum values gradually decreases, the fluctuation in P_{32} values significantly decreases, and the spatial effect considerably weakens. The fluctuation in the P_{32} values tends to stabilize when the cube size is greater than or equal to a critical value.

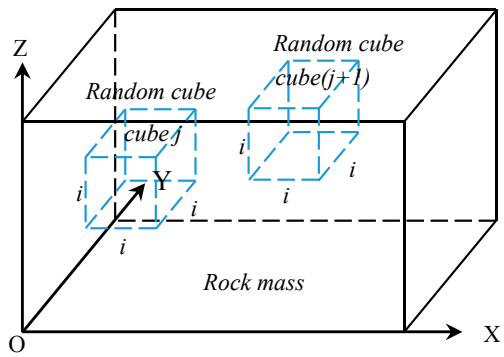

Figure 6. The randomly distributed cubes in a fractured rock mass.

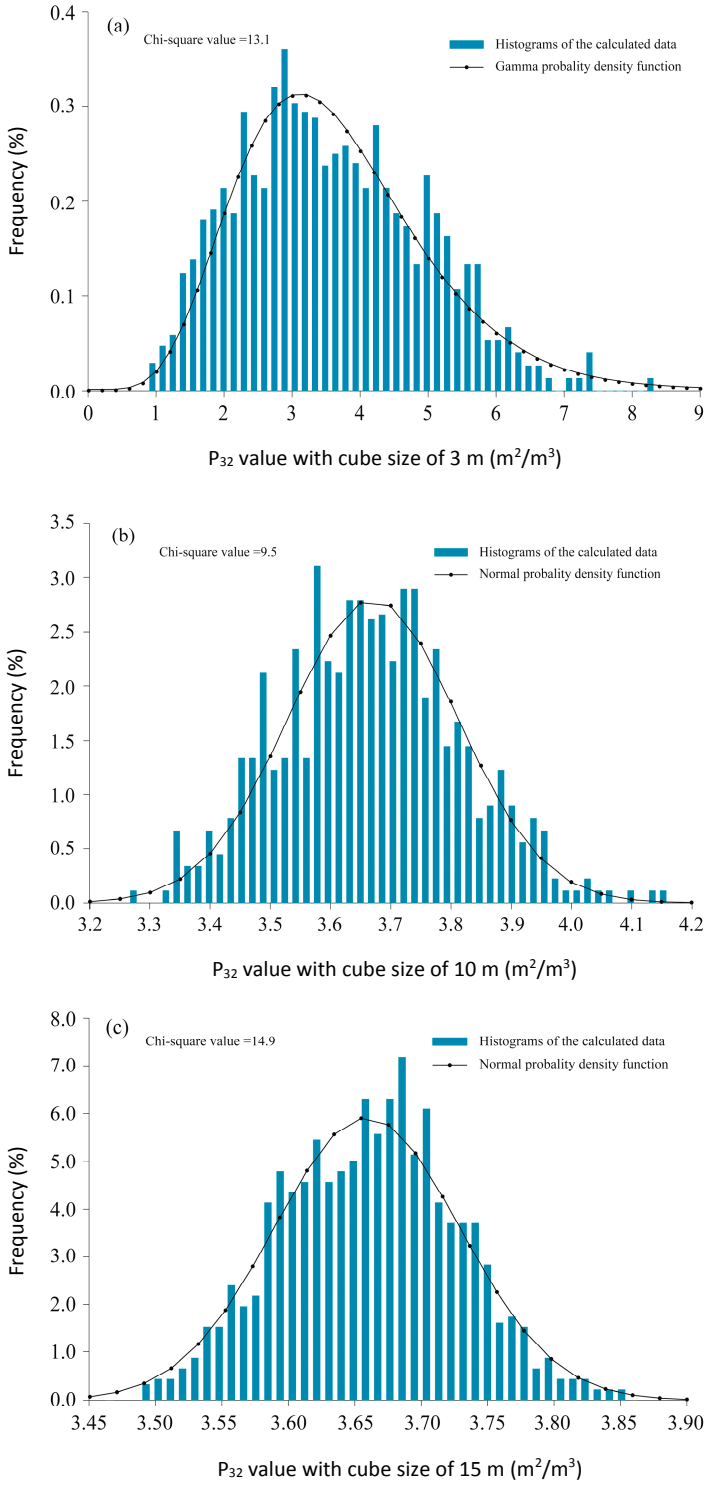

Figure 7. The frequency histograms of the volumetric fracture intensity P_{32} for three cube sizes. (**a**) cube size of 3 m. (**b**) cube size of 10 m. (**c**) cube size of 15 m.

The fractures were randomly distributed in the generated 3D fracture network model. When we evaluate the structural properties of the rock masses, the spatial effects should be considered [34]. Figure 8 shows that, in different regions, the P_{32} values from the same cube size differ within a certain range, and the spatial effects weaken as the cube size increases. Therefore, considering both the size effect and the spatial effect is necessary to determine the REV size.

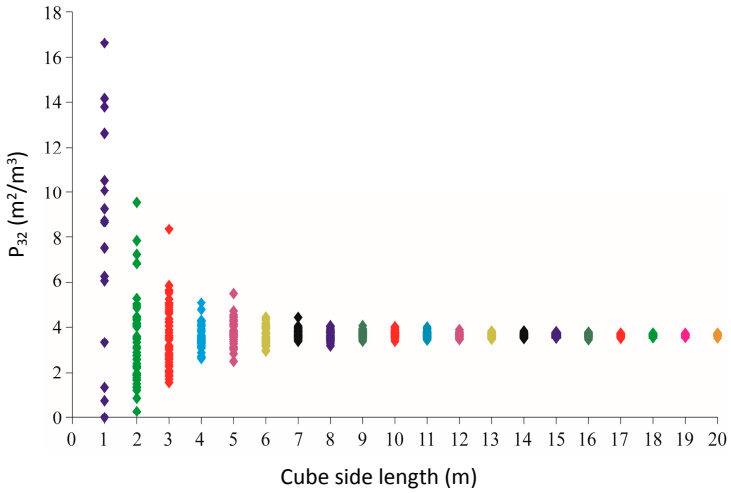

Figure 8. The volumetric fracture intensity for different cube sizes.

Table 3. The results of the chi-square goodness-of-fit tests for each sample.

Cube Size (m)	Chi-Square Goodness-of-Fit Test			Cube Size (m)	Chi-Square Goodness-of-Fit Test		
	Critical Chi-Square Value	Minimum Chi-Square Value	Distribution Form		Critical Chi-Square Value	Minimum Chi-Square Value	Distribution Form
1	21.0	19.1	Lognormal	11	21.0	19.1	Lognormal
2	21.0	15.0	Gamma	12	21.0	17.3	Lognormal
3	21.0	13.1	Gamma	13	21.0	18.7	Normal
4	21.0	16.9	Lognormal	14	21.0	13.1	Normal
5	21.0	10.9	Lognormal	15	21.0	14.9	Normal
6	21.0	11.3	Lognormal	16	21.0	12.3	Lognormal
7	21.0	11.2	Lognormal	17	21.0	10.5	Lognormal
8	21.0	16.1	Normal	18	19.7	6.3	Triangle
9	21.0	8.6	Lognormal	19	19.7	14.4	Triangle
10	21.0	9.5	Normal	20	19.7	11.2	Triangle

4.2. REV Size Based on Statistical Tests

In a fractured rock mass, the number of fractures increases with the sample size [23]. The relationship between the area of fractures and the volume of the rock mass was quantified by the volumetric fracture intensity P_{32}. Therefore, it is necessary to determine the geometrical REV size by considering the fracture intensity characteristics in the fractured rock mass. The REVs were obtained from 100 random regions by using the method of Kanit et al. [62]. As shown in Figure 9, the REV values fluctuate with the study regions. Generally, the REV value in a certain region cannot exactly represent the REV of the entire rock mass. To obtain a more reasonable REV size, the anisotropy of rock masses and comprehensive differences between different methods should be seriously considered. Therefore, using several statistical methods to comprehensively determine the REV size is necessary [34]. In this paper, a method was presented to estimate the geometrical REV size based on the volumetric fracture intensity P_{32} and statistical tests. The properties of the size effect and spatial effect for fractured rock masses were studied using the calculated P_{32} values, which depended on the fracture disc characteristics in the 3D fracture network model. To describe the uncertainty in our reported P_{32} values, the confidence interval of each dataset is calculated. As shown in Figure 10, the error bars represent a particular confidence interval with a 95% confidence level. The fluctuation of P_{32} values significantly decreases with cube sizes varying from 1 to 20 m. Subsequently, the REVs were estimated by calculating P_{32} values and the two statistical test methods reported in Section 3. The P_{32} values for sample 20 compared with those of the sample sizes varying from 1 to 19, and a 5% significance level was used to determine whether two samples are statistically similar.

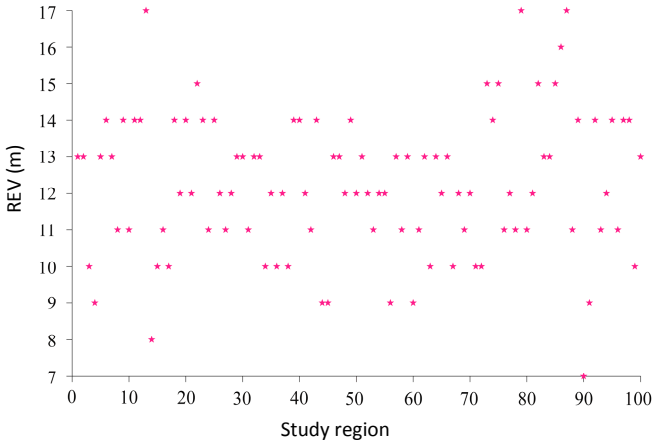

Figure 9. The REV values varied with the study regions.

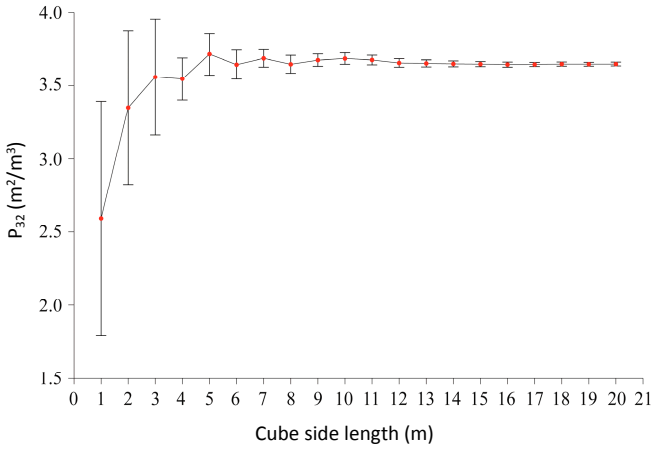

Figure 10. The error bar chart with confidence interval for different datasets.

The likelihood ratio test and Wald–Wolfowitz runs test were used to determine the geometrical REV size based on the P_{32} values for different sample sizes. The results of the statistical tests for the volumetric fracture intensity P_{32} values are summarized in Table 4. The null hypothesis does not lead to a rejection when the *p* value is greater than or equal to the significance level of 0.05. The larger the *p* value is, the greater the likelihood that the two compared samples are statistically similar. Table 4 shows that the *p* value increased with the cube size of the sample, the similarity degree between two samples increased with the cube size of the sample, and the fluctuation in the volumetric fracture intensity P_{32} values decreased significantly.

The Wald–Wolfowitz runs test demonstrated that the null hypothesis could not be rejected when the sample size is larger than or equal to 13 m, but the likelihood ratio test demonstrated that the null hypothesis was accepted when the sample size was larger than or equal to 12 m. Therefore, the geometrical REV size was determined to be 13 m using the Wald–Wolfowitz runs test, but the geometrical REV size was determined to be 12 m using the likelihood ratio test. The REV size based on the Wald–Wolfowitz runs test was larger than that of the likelihood ratio test. Different results were obtained for these two statistical test methods that consider different aspects. The likelihood ratio test focuses on the likelihood ratio, which expresses how many times more likely the data are under one model than the other, whereas the Wald–Wolfowitz runs test focuses on the randomness of the sequence for two independent sample data. Therefore, it is necessary to determine a more reasonable REV size by considering the comprehensive difference between different methods. Finally, considering

a result that both the likelihood ratio test and Wald–Wolfowitz runs test accept, the larger cube size, 13 m, is selected as the geometrical REV size of the fractured rock mass at the Maji dam site in China.

Table 4. Results of the likelihood ratio test and Wald–Wolfowitz runs test.

Cube Size of Sample (m)	Cube Size of Sample 20 (m)	Likelihood Ratio Test		Wald–Wolfowitz Runs Test	
		p Value	Result	*p* Value	Result
1	20	7.48×10^{-76}	Reject	4.49×10^{-64}	Reject
2	20	4.50×10^{-90}	Reject	3.43×10^{-44}	Reject
3	20	2.26×10^{-117}	Reject	3.46×10^{-39}	Reject
4	20	9.24×10^{-116}	Reject	3.46×10^{-39}	Reject
5	20	1.56×10^{-84}	Reject	1.37×10^{-37}	Reject
6	20	1.68×10^{-47}	Reject	1.70×10^{-34}	Reject
7	20	3.44×10^{-55}	Reject	9.13×10^{-25}	Reject
8	20	1.99×10^{-15}	Reject	9.95×10^{-29}	Reject
9	20	4.06×10^{-17}	Reject	1.30×10^{-9}	Reject
10	20	5.72×10^{-9}	Reject	7.09×10^{-9}	Reject
11	20	5.76×10^{-5}	Reject	1.14×10^{-4}	Reject
12	20	0.059	Accept	0.001	Reject
13	20	0.136	Accept	0.500	Accept
14	20	0.154	Accept	0.285	Accept
15	20	0.423	Accept	0.976	Accept
16	20	0.594	Accept	0.715	Accept
17	20	0.899	Accept	0.899	Accept
18	20	0.809	Accept	0.844	Accept
19	20	0.877	Accept	0.761	Accept

5. Discussion

5.1. Investigation of the REV Size

Many methods have been developed for the REV research of fractured rock masses, which can be divide into three categories in terms of the research viewpoints of relevant parameters: the geometrical parameters of discontinuities and rock blocks, and the mechanical and hydraulic parameters of the fractured rock mass. The quantitative indicators of geometrical REVs mainly focus on the geometrical parameters, such as trace length, fracture orientation, fracture intensity, and fracture connectivity [1,17,19,21,23,32–36]. Based on the aforementioned geometrical parameters, many statistical methods have been used to estimate the geometrical REV sizes. The mechanical REVs mainly focus on the mechanical parameters of the fractured rock mass, such as elastic modulus, Poisson's ratio, stiffness modulus, and damage coefficient [15,19,23]. However, due to the limitation of site conditions and high costs of large in situ test, the laboratory rock mechanics test and numerical simulation technology are always used to determine mechanical REVs of fractured rock masses using numerical software, such as PFC application [19,22,23]. The REVs obtained from hydraulic parameters mainly focus on the hydraulic properties of the fractured rock mass, such as hydraulic conductivity and equivalent permeability tensor [4,5,63,64]. Based on the aforementioned methods, it can be seen that the different methods focus on different aspects, and the REVs obtained from different methods are not identical [19,23,64]. Even though we employed the same method to estimate the REVs, the REV values obtained from different parameters are not exactly the same [32,35,36]. Therefore, it is necessary to consider comprehensive difference and to determine a more reasonable REV size by using different methods. Generally, it is relatively simple and feasible to calculate REV size by using the geometrical parameter and several different statistical methods. However, it is relatively complex to calculate REV values by using the mechanical and hydraulic parameters. Especially, multiple parameters are considered at the same time. Therefore, in future research, we still need to further explore the REVs by considering different aspects.

5.2. Geometrical REV Calculation

In this work, based on the field survey at the Maji dam site, we established a relatively reasonable process for calculating geometrical REVs. Based on the current investigation of geometrical REVs, the calculation procedure is described as follows:

1. Generate a reliable 3D fracture network model based on the joint data obtained from the field survey.
2. Select several random regions in the generated 3D fracture network model.
3. Calculate the geometrical parameters of fractured rock masses by varying cube sizes and locations. Generally, the fracture intensity index is widely applied.
4. Generate n samples with the same cube size, which vary from 1 to n m.
5. Analyze the REV size by using several different statistical test methods.

In this paper, the proposed method comprehensively considers the anisotropy of rock masses, simplicity of calculation and differences between different methods. Specifically, the volumetric fracture intensity P_{32} and two statistical test methods (i.e., the likelihood ratio test and Wald–Wolfowitz runs test) were adopted to estimate the REV sizes at the dam site of Maji hydropower station. Because different parameters and methods have different considerations and impact factors, the REVs obtained from these parameters and methods may be varied. To ensure a result that both the likelihood ratio test and Wald–Wolfowitz runs test accept, we select the larger critical value as the REV of the studied rock mass.

6. Conclusions

This paper presents a method for estimating the geometrical representative element volume of the fractured rock mass based on the volumetric fracture intensity P_{32} and two statistical tests. It was demonstrated that this method was used to calculate the volumetric fracture intensity P_{32} and determine the geometrical REV size at the Maji dam site in China.

The field fracture data were collected by using the rectangular window sampling method. A 150 m $\times$ 80 m $\times$ 50 m 3D fracture network model was generated to calculate the geometrical REV size of the studied rock masses. The volumetric fracture intensity P_{32} values were determined based on the 3D fracture network model in random regions for cube side lengths ranging from 1 to 20 m. The results show that the distribution of the P_{32} values for each cube size is different. The size effect and spatial effect are very significant; the P_{32} values from the same sample sizes at different locations vary; as the sample size increases, the change in P_{32} values reduces gradually, and the fluctuation in P_{32} values decreases significantly.

To consider the anisotropic characteristics of a rock mass and comprehensive differences between different methods, the likelihood ratio test and Wald–Wolfowitz runs test were used to discuss the geometrical REV size of fractured rock masses. A 5% significance level was selected to estimate the statistical similarity between two sample volumes. Subsequently, the geometrical REV size was defined as 13 m using the Wald–Wolfowitz runs test method, but the geometrical REV size was defined as 12 m using the likelihood ratio test. Considering that different test methods emphasize different considerations and impact factors, the larger cube size, 13 m, was chosen. Finally, the geometrical REV size of the fractured rock mass was determined to be 13 m at the Maji dam site in China. In this study, the larger fractures were not involved in the computation, and the location of the fracture centroid is assumed to obey a homogeneous Poisson process. If the larger fractures cannot be ignored or the hypothesis is not set up, the REV size may strongly increase or cannot be found. Therefore, we should identify and deal with such cases in the future research.

Author Contributions: Y.L.: Article writing, 3D fracture network model establishment; Q.W.: 3D fracture network model establishment and design of the work; J.C.: 3D fracture network model establishment and design of the work; S.S.: Data collection and analysis; J.Z.: Data analysis and revising the manuscript; X.H.: Data collection and revising the manuscript.

Acknowledgments: This work was supported by the key project of National Natural Science Foundation of China (Grant No. 41330636), the National Natural Science Foundation of China (Grant No. 41702301), China Postdoctoral Science Foundation (Grant No. 2017M611324) and the Graduate Innovation Fund of Jilin University (Grant No. 2017137).

Conflicts of Interest: The authors declare no conflict of interest.

References

1. Song, S.Y.; Sun, F.Y.; Chen, J.P.; Zhang, W.; Han, X.D.; Zhang, X.D. Determination of RVE size based on the 3D fracture persistence. *Q. J. Eng. Geol. Hydrogeol.* **2017**, *50*, 60–68. [CrossRef]
2. Bear, J. *Dynamics of Fluids in Porous Media*; American Elsevier: New York, NY, USA, 1972.
3. Long, J.C.S.; Remer, J.S.; Wilson, C.R.; Witherspoon, P.A. Porous media equivalents for networks of discontinuous fractures. *Water Resour. Res.* **1982**, *18*, 645–658. [CrossRef]
4. Kulatilake, P.H.S.W.; Panda, B.B. Effect of block size and joint geometry on jointed rock hydraulics and REV. *J. Eng. Mech.* **2000**, *126*, 850–858. [CrossRef]
5. Wang, M.; Kulatilake, P.H.S.W.; Um, J.; Narvaiz, J. Estimation of REV size and three-dimensional hydraulic conductivity tensor for a fractured rock mass through a single well packer test and discrete fracture fluid flow modeling. *Int. J. Rock Mech. Min. Sci.* **2002**, *39*, 887–904. [CrossRef]
6. Zhang, D.; Zhang, R.; Chen, S.; Soll, W.E. Pore-scale study of flow in porous media: Scale dependency, REV, and statistical REV. *Geophys. Res. Lett.* **2000**, *27*, 1195–1198. [CrossRef]
7. Al-Raoush, R.; Papadopoulos, A. Representative elementary volume analysis of porous media using X-ray computed tomography. *Powder Technol.* **2010**, *200*, 69–77. [CrossRef]
8. Shah, S.M.; Crawshaw, J.P.; Gray, F.; Yang, J.; Boek, E.S. Convex hull approach for determining rock representative elementary volume for multiple petrophysical parameters using pore-scale imaging and Lattice—Boltzmann modelling. *Adv. Water Resour.* **2017**, *104*, 65–75. [CrossRef]
9. Tóth, T.M.; Vass, I. Relationship between the geometric parameters of rock fractures, the size of percolation clusters and REV. *Math. Geosci.* **2011**, *43*, 75–97. [CrossRef]
10. Neuman, S.P. Stochastic continuum representation of fractured rock permeability as an alternative to the REV and fracture network concepts. In Proceedings of the 28th US Symposium of Rock Mechanics, University of Arizona, Tucson, AZ, USA, 29 June–1 July 1987; pp. 533–561.
11. Pinto, A.; Da, C.H. *Scale Effects in Rock Mechanics*; A.A. Balkema Publishers: Rotterdam, The Netherlands, 1993.
12. Kulatilake, P.H.S.W. Estimating elastic constants and strength of discontinuous rock. *J. Geotech. Eng.* **1985**, *111*, 847–864. [CrossRef]
13. Pariseau, W.G.; Puri, S.; Schmelter, S.C. A new model for effects of impersistent joint set on rock slope stability. *Int. J. Rock Mech. Min. Sci.* **2008**, *45*, 122–131. [CrossRef]
14. Chalhoub, M.; Pouya, A. Numerical homogenization of a fractured rock mass: A geometrical approach to determine the mechanical representative elementary volume. Electron. *J. Geotech. Eng.* **2008**, *13*, 1–12.
15. Castelli, M.; Saetta, V.; Scavia, C. Numerical study of scale effects on the stiffness modulus of rock masses. *Int. J. Geomech.* **2003**, *3*, 160–169. [CrossRef]
16. Min, K.B.; Jing, L. Numerical determination of the equivalent elastic compliance tensor for fractured rock masses using the distinct element method. *Int. J. Rock Mech. Min. Sci.* **2003**, *40*, 795–816. [CrossRef]
17. Baghbanan, A.; Jing, L. Hydraulic properties of fractured rock masses with correlated fracture length and aperture. *Int. J. Rock Mech. Min. Sci.* **2007**, *44*, 704–719. [CrossRef]
18. Khani, A.; Baghbanan, A.; Hashemolhosseini, H. Numerical investigation of the effect of fracture intensity on deformability and REV of fractured rock masses. *Int. J. Rock Mech. Min. Sci.* **2013**, *63*, 104–112. [CrossRef]
19. Ni, P.; Wang, S.; Wang, C.; Zhang, S. Estimation of REV Size for Fractured Rock Mass Based on Damage Coefficient. *Rock Mech. Rock Eng.* **2017**, *50*, 555–570. [CrossRef]
20. Li, G.; Tang, C.A. A statistical meso-damage mechanical method for modeling trans-scale progressive failure process of rock. *Int. J. Rock Mech. Min. Sci.* **2015**, *74*, 133–150. [CrossRef]
21. Lu, B.; Ge, X.R.; Zhu, D.L.; Chen, J.P. Fractal study on the representative element volume of jointed rock masses. Chin. *J. Rock Mech. Eng.* **2005**, *24*, 1355–1361.

22. Pierce, M.; MasIvars, D.; Cundall, P.A.; Potyondy, D. A synthetic rock mass model for jointed rock. In Proceedings of the First CA-US Rock Mechanics Symposium, Vancouver, BC, Canada, 27–31 May 2007; pp. 341–349.
23. Esmaieli, K.; Hadjigeorgiou, J.; Grenon, M. Estimating geometrical and mechanical REV based on synthetic rock mass models at Brunswick Mine. *Int. J. Rock Mech. Min. Sci.* **2010**, *47*, 915–926. [CrossRef]
24. Xia, L.; Zheng, Y.H.; Yu, Q.C. Estimation of the REV size for blockiness of fractured rock masses. *Comput. Geotech.* **2016**, *76*, 83–92. [CrossRef]
25. Oda, M. A new method for evaluating the representative elementary volume based on joint survey of rock masses. *Can. Geotech. J.* **1988**, *25*, 440–447. [CrossRef]
26. Li, J.H.; Zhang, L.M. Geometric parameters and REV of a crack network in soil. *Comput. Geotech.* **2010**, *37*, 466–475. [CrossRef]
27. Lama, R.D.; Vutukuri, V.S. *Handbook on Mechanical Properties of Rocks-Testing Techniques and Results, Vol. 2*; Monograph, Series on Rock and Soil Mechanics, Vol. 3, No. 1; Trans Tech Publications: Bay Village, OH, USA, 1978; p. 495.
28. Schultz, R.A. Relative scale and the strength and deformability of rock masses. *J. Struct. Geol.* **1996**, *18*, 1139–1149. [CrossRef]
29. Elmo, D.; Stead, D. An integrated numerical modelling—discrete fracture network approach applied to the characterization of rock mass strength of naturally fractured pillars. *Rock Mech. Rock Eng.* **2010**, *43*, 3–19. [CrossRef]
30. Einstein, H.H.; Locsin, J.L.Z. Modeling rock fracture intersections and application to the Boston area. *J. Geotech. Geoenviron. Eng.* **2012**, *138*, 1415–1421. [CrossRef]
31. Ivanova, V.M.; Sousa, R.; Murrihy, B.; Einstein, H.H. Mathematical algorithm development and parametric studies with the GEOFRAC three-dimensional stochastic model of natural rock fracture systems. *Comput. Geosci.* **1997**, *67*, 100–109. [CrossRef]
32. Zhang, W.; Chen, J.P.; Liu, C.; Huang, R.; Li, M.; Zhang, Y. Determination of geometrical and structural representative volume elements at the Baihetan dam site. *Rock Mech. Rock Eng.* **2012**, *45*, 409–419. [CrossRef]
33. Zhang, W.; Chen, J.P.; Cao, Z.X.; Wang, R.Y. Size effect of RQD and generalized representative volume elements: A case study on an underground excavation in Baihetan dam, Southwest China. *Tunn. Undergr. Space Technol.* **2013**, *35*, 89–98. [CrossRef]
34. Zhang, W.; Chen, J.P.; Chen, H.E.; Xu, D.Z.; Li, Y. Determination of RVE with consideration of the spatial effect. *Int. J. Rock Mech. Min. Sci.* **2013**, *61*, 154–160. [CrossRef]
35. Zhang, W.; Chen, J.P.; Yuan, X.Q.; Xu, P.H.; Zhang, C. Analysis of RVE size based on three-dimensional fracture numerical network modelling and stochastic mathematics. *Q. J. Eng. Geol. Hydrogeol.* **2013**, *46*, 31–40. [CrossRef]
36. Li, Y.; Chen, J.P.; Shang, Y.J. Determination of the geometrical REV based on fracture connectivity: A case study of an underground excavation at the Songta dam site, China. *Bull. Eng. Geol. Environ.* **2017**. [CrossRef]
37. Kulatilake, P.H.S.W.; Wu, T.H. Estimation of mean trace length of discontinuities. *Rock Mech. Rock Eng.* **1984**, *17*, 215–232. [CrossRef]
38. Baecher, G.B.; Lanney, N.A.; Einstein, H.H. Statistical description of rock properties and sampling. In Proceedings of the 18th Symposium on Rock Mechanics, Colorado School of Mines, Golden, Colorado, 22–24 June 1977; American Institute of Mining Engineers: New York, NY, USA, 1977; pp. 1–8.
39. Priest, S.D. *Discontinuity Analysis for Rock Engineering*; Chapman & Hall: London, UK, 1993.
40. Chen, J.P.; Xiao, S.F.; Wang, Q. *Three Dimensional Network Modeling of Stochastic Fractures*; Northeast Normal University Press: Changchun, China, 1995.
41. Li, Y.; Wang, Q.; Chen, J.P.; Xu, L.M.; Song, S.Y. K-means algorithm based on particle swarm optimization for the identification of rock discontinuity sets. *Rock Mech. Rock Eng.* **2015**, *48*, 375–385. [CrossRef]
42. Fisher, R.A. Dispersion on a sphere. *Proc. R. Soc. A* **1953**, *217*, 295–305. [CrossRef]
43. Bingham, C. Distributions on the Sphere and on the Projective Plane. Ph.D. Thesis, Yale University, New Haven, CT, USA, 1964.
44. Marcotte, D.; Henry, E. Automatic joint set clustering using a mixture of bivariate normal distributions. *Int. J. Rock Mech. Min. Sci.* **2002**, *39*, 323–334. [CrossRef]
45. Chen, J.P.; Shi, B.F.; Wang, Q. 3-D network numerical modeling technique for random discontinuities of rock mass. *Chin. J. Geotech. Eng.* **2001**, *23*, 397–402.

46. Han, X.D.; Chen, J.P.; Wang, Q.; Li, Y.; Zhang, W.; Yu, T. A 3D fracture network model for the undisturbed rock mass at the Songta dam site based on small samples. *Rock Mech. Rock Eng.* **2016**, *49*, 611–619. [CrossRef]
47. Kulatilake, P.H.S.W.; Wu, T.H. Sampling bias on orientation of discontinuities. *Rock Mech. Rock Eng.* **1984**, *17*, 243–253. [CrossRef]
48. Warburton, P.M. A stereological interpretation of joint trace data. *Int. J. Rock Mech. Min. Sci. Geomech. Abstr.* **1980**, *17*, 181–190. [CrossRef]
49. Zhang, L.; Einstein, H.H. Estimating the intensity of rock discontinuities. *Int. J. Rock Mech. Min. Sci.* **2000**, *37*, 819–837. [CrossRef]
50. Karzulovic, A.; Goodman, R.E. Determination of principal joint frequencies. *Int. J. Rock Mech. Min. Sci. Geomech. Abstr.* **1985**, *22*, 471–473. [CrossRef]
51. Oda, M. Fabric tensor for discontinuous geological materials. *Soil Found.* **1982**, *22*, 96–108. [CrossRef]
52. Kulatilake, P.H.S.W.; Wathugala, D.N.; Stephansson, O. Joint network modeling including a validation to an area in Stripa Mine, Sweden. *Int. J. Rock Mech. Min. Sci. Geomech. Abstr.* **1993**, *30*, 503–526. [CrossRef]
53. Kulatilake, P.H.S.W.; Um, J.; Wang, M.; Escandon, R.F.; Narvaiz, J. Stochastic fracture geometry modeling in 3-D including validations for a part of Arrowhead East Tunnel, California, USA. *Eng. Geol.* **2003**, *70*, 131–155. [CrossRef]
54. Dershowitz, W.S.; Herda, H.H. Interpretation of fracture spacing and intensity. In Proceedings of the 33rd US Rock Mechanical Symposium, Santa Fe, NM, USA, 3–5 June 1992.
55. Xu, C.; Dowd, P. A new computer code for discrete fracture network modelling. *Comput. Geosci.* **2010**, *36*, 292–301. [CrossRef]
56. Zheng, J.; Deng, J.H.; Zhang, G.Q.; Yang, X.J. Validation of Monte Carlo simulation for discontinuity locations in space. *Comput. Geotech.* **2015**, *67*, 103–109. [CrossRef]
57. Huelsenbeck, J.P.; Crandall, K.A. Phylogeny estimation and hypothesis testing using maximum likelihood. *Ann. Rev. Ecol. Syst.* **1997**, *28*, 437–466. [CrossRef]
58. Wilks, S.S. The large-sample distribution of the likelihood ratio for testing composite hypotheses. *Ann. Math. Stat.* **1938**, *9*, 60–62. [CrossRef]
59. Wald, A.; Wolfowitz, J. On a test whether two samples are from the same population. *Ann. Math. Stat.* **1940**, *11*, 147–162. [CrossRef]
60. Friedman, J.H.; Rafsky, L.C. Multivariate generalizations of the Wald-Wolfowitz and Smirnov two-sample testing. *Ann. Stat.* **1979**, *7*, 697–717. [CrossRef]
61. Zhan, J.W.; Chen, J.P.; Xu, P.H.; Han, X.D.; Chen, Y.; Ruan, Y.K.; Zhou, X. Computational framework for obtaining volumetric fracture intensity from 3D fracture network models using Delaunay triangulations. *Comput. Geotech.* **2017**, *89*, 179–194. [CrossRef]
62. Kanit, T.; Forest, S.; Galliet, I.; Mounoury, V.; Jeulin, D. Determination of the size of the representative volume element for random composites: Statistical and numerical approach. *Int. J. Solids Struct.* **2003**, *40*, 3647–3679. [CrossRef]
63. Min, K.B.; Jing, L.; Stephansson, O. Determining the equivalent permeability tensor for fractured rock masses using a stochastic REV approach: Method and application to the field data from Sellafield, UK. *Hydrogeol. J.* **2004**, *12*, 497–510. [CrossRef]
64. Wang, Z.C.; Li, W.; Bi, L.P.; Qiao, L.P.; Liu, R.C.; Liu, J. Estimation of the REV Size and Equivalent Permeability Coefficient of Fractured Rock Masses with an Emphasis on Comparing the Radial and Unidirectional Flow Configurations. *Rock Mech. Rock Eng.* **2018**, *6*, 1–15. [CrossRef]